GWP-FRACTURE

V. 1.0

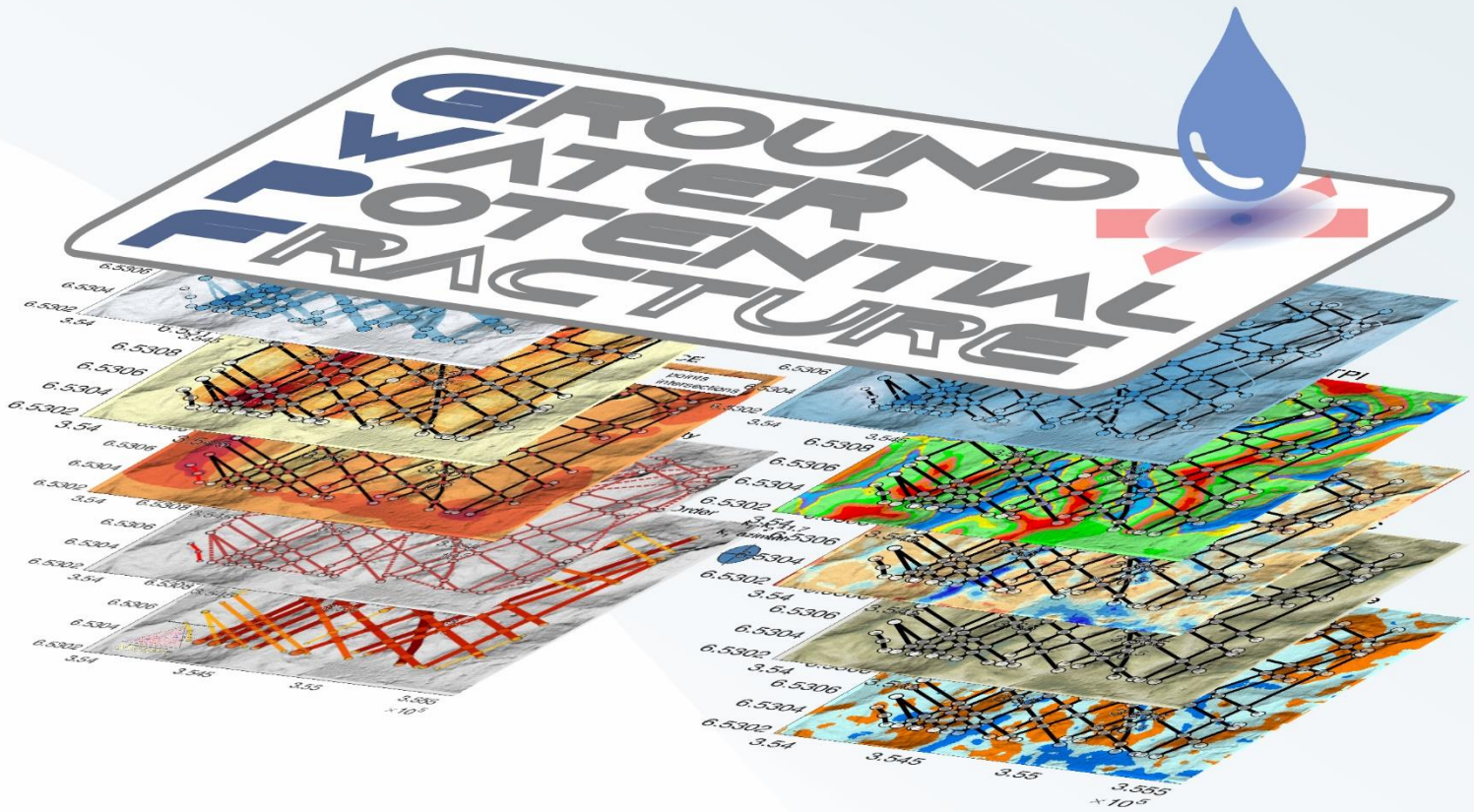

QUICK USER GUIDE

Version 1.0, November 2019
García Aráoz
egarciaaraoz@conicet.gov.ar.com

Note: GWP-Fracture needs MATLAB Compiler Runtime to be installed first.

Contenido

1. About GWP-Fracture

GWP-Fracture is a new MATLAB™ application based on Multi-Criteria Decision Analysis and Analytic Hierarchy Process (MCDA-AHP) techniques for groundwater potential delineation of hard rock environments. The software has been created to assist in the design of field campaigns during the early stages of exploration, especially in regions where information is lacking or not available.

GWP-Fracture has been tested with different data sets from a wide range of spatial scales, rock types and tectonic settings. In all cases, it has been observed that in order to obtain reliable results it is necessary to correctly select the input data and the weights assigned to each variable during the analysis process. In this sense, the hydrogeological criterion and the previous experience of the operator becomes fundamental in the whole process.

In all cases, the software has proved to be an efficient tool, simple to apply and interpret, and low cost. The results obtained by GWP-Fracture can be very useful for preliminary prospecting studies or feasibility studies in areas where there is little or no record of previous hydrogeological studies, allowing to reduce campaign costs to implement more complex prospecting techniques.

The decision to implement GWP-Fracture in MATLAB™, and not another coding language such as Python or C++, was based on a number of factors, including general availability, and familiarity with MATLAB™ among geologists researchers, a wide range of useful built-in functions in the various add-on Toolboxes (e.g. for Image Processing, and Statistics), and relative ease of use.

GWP-Fracture uses code written by others authors: cmocean.m by Chad A.; circStat.m, getConnectivity.m, guiFracPaQ2Dtensor.m, intensity.m, plotEllipse.m, probeplane.m, roseEqualAreaColour.m, triplot.m and tripts.m from the FracPaQ toolbox by Dave Healy (Healy et al., 2017); boundingBox.m, distancePointEdge.m, distancePointPolyline.m, distancePoints.m, isPointOnPolyline.m, polygonArea.m, polygonCentroid.m and polylineLenght.m from the package geom2d by David Legland; lineSegmentIntersect.m by Murat Erdem; densityplot.m by Changyong HE; fuzzAHP2.m and RI by Demet Cilden & Dogus Guler; idw.m by Andres Tovar; intersections.m by Douglas M. Schwarz; labelpoints.m by Adam Danz; mploy2mask.m by Steve Eddins; ndnanfilter.m by Carlos Adrian Vargas Aguilera; offsetCurve.m by J. Duchateau; slope2.m by Chad A. Greene; othercolor.m by Joshua Atkins; builtincaller.m, copy2GRIDobj.m, fillsinks.m, flowacc.m, FLOWobj.m, GRIDobj.m, GRIDobj2geotiff.m, GRIDobj2mat.m, hillshade.m, identifyflats.m, imageschs.m, log.m, minus.m, plus.m, rdivide.m, refmat2XY.m, validatealignment.m from the TopoToolbox toolbox by Wolfgang Schwanghart (Schwanghart and Kuhn, 2010; Schwanghart and Scherler, 2014). The handling of image file output in GWP-Fracture also uses functions from the Image Processing Toolbox, a MATLAB™ add-on.

GWP-Fracture totals over 5,000 lines of code. As in any software project of this scale, there will be 'bugs' – i.e. coding errors. If you encounter a bug, please let us know, through GitHub, Mathworks™ FileExchange or by e-mail (egarciaaraoz@conicet.gov.ar.com); please provide as many details as you can, including (where possible) a screen shot of the error, the input file you were using at the time, and the MATLAB™ version.

2. General assumptions

The rationale behind the development of GWP-Fracture has been to create a methodological tool that allows users to make hydrogeological deductions of hard rocks environments (applicable even in inaccessible areas) in a simple, fast and inexpensive way from freely accessible information. This means that field data or complex survey techniques are not required. In order to prioritize this objective, only two inputs are required in the app: map lineaments and topography. Thus, some general simplifications and assumptions must be made:

-The hydrogeological conceptual model of hard rocks environment typically consists of three vertical zones: upper weathered, middle fractured and deep massive (Sharp, 2014). This vertical sequence is common but, under specific conditions, the upper-weathered zone can be missing (e.g. due to erosive processes) or have a thickness and extension that are insufficient to accommodate aquifers with good and sustainable flow over time, (e.g., aquifers restricted to small valleys). In such cases, these aquifers can be very dependent on direct rainfall and consequently very vulnerable to dry periods. Therefore, the aquifer that may be of greatest interest, from the point of view of possibilities of permanent water catchment over time will be in the middle zone and the deep zone, where the greatest number of discontinuities are found.

-The rock massif is considered as an impermeable discontinuous medium, where the circulation and storage of water occurs only in favor of discontinuities. Discontinuities are the most important hydrogeological property of hard rocks because they are common to all of them independently of their great variety of mineralogy, petrology, and stratigraphy (Gustafsson, 1994), giving the rock most of the porosity and effective permeability. Therefore, whether in the form of fractures, joints, geological contacts, shear zones, faults, vugs and/or other discontinuities, these will control the groundwater pathways (Chandra et al., 2019; Schneeberger et al., 2018).

- Discontinuities can be sorted according to an order of magnitude, which is a function of trace length (Jafari and Babadagli, 2011, 2009; Liu et al., 2016). It is assumed that discontinuities with longer and persistent traces are associated with areas of greater weakness and therefore greater permeability. According to Barrocu (2007), fractures which are much longer, are potentially good groundwater reservoirs and collectors of the water stored in the smaller fractures communicating with them.

-Surface roughness, aperture, curvature and filling material of fractures are not currently considered. These characteristics are assumed to be the same for all discontinuities or to be directly proportional to the order of magnitude of the discontinuities.

-The position and orientation of the discontinuity in relation to topography determines their infiltration capacity.

-The input map lineaments lie on a statistically flat 2D surface, where topography does not affect the appearance of any fracture trace trajectories.

This model is practical at the expense of rigour. These simplifying assumptions can reduce the generality of the results. However, it is easy to implement and retains enough of the character of real hydrogeological aspects of hard rock environments.

3. Installation

For MATLAB™ users the application can be installed by copying all of the files from the GitHub repositories (https://github.com/garciaaraoze/GWP-Fracture) into a folder on the user's computer. After starting MATLAB™, the working directory should be set to the folder containing the source code and sample files. The application is started by typing 'GWPFracture' in the command window of a MATLAB™ session.

For other users, the app is available at GitHub (https://github.com/garciaaraoze/GWP-Fracture). The current version of GWP-Fracture needs MATLAB Compiler Runtime 9.4 (MCR 9.4) to be installed first, while the app itself can be run without any extra installation. MCR 9.4 can be downloaded for free from the MathWorks website (https://la.mathworks.com/products/compiler/matlab-runtime.html).

After starting GWP-Fracture the user has to be patient for at least 60 s, as the MCR 9.4 has to be launched in the background. Optionally, all running processes on the computer can be checked via the task manager of the system software.

4. Inputs data

Only two inputs are required in the app: lineaments maps in shape format (*.shp) and DEM in raster geotiff format (*.tif).

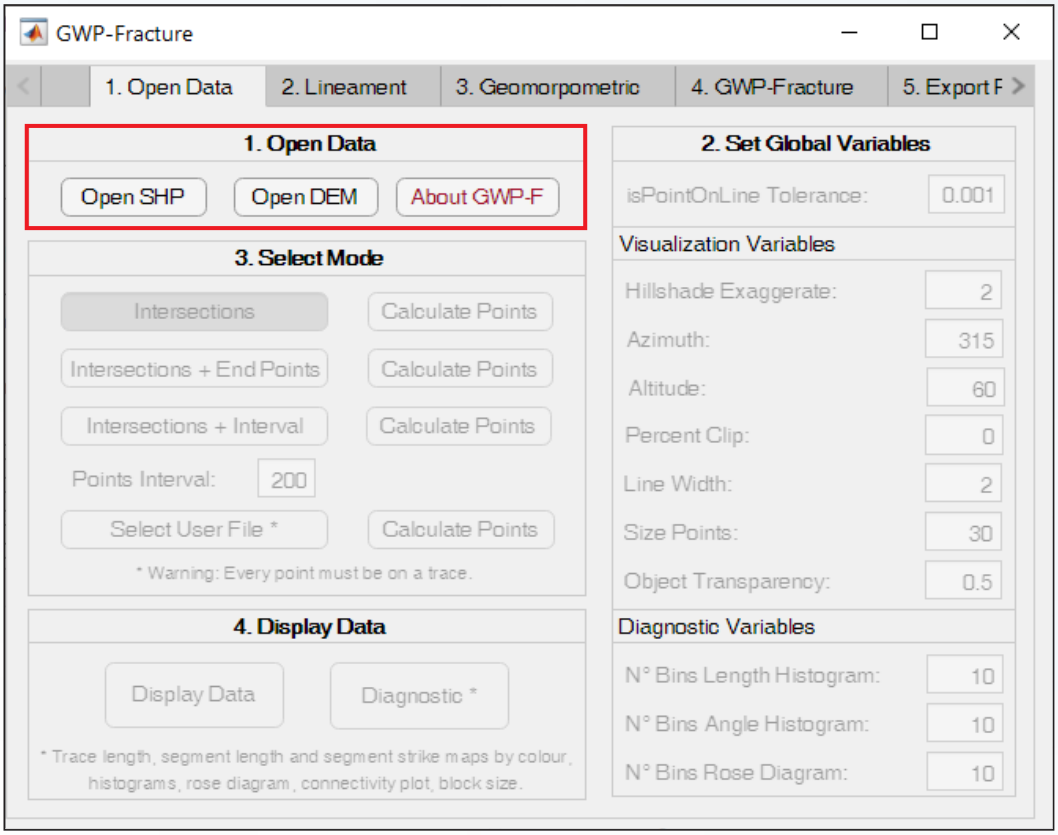

Figure1: Loading data.

Note that both files must be in the same planar projected coordinate system (i.e., UTM) because the software does not support geographic coordinates or allow to change projections.

It is important to emphasize the importance of preliminary recognition and photo-interpretation studies since, when hydrogeological data are not available, they are practically the only starting point for making hydrogeological deductions. The operator must get into the habit of considering the problems of groundwater location and movement when examining the aerial photograph of the study area, in order to draw the lineament's map.

The mapping of the lineaments should be done with a solid hidrogeological criterion and it is recommended that the size of the mapped area be larger than the area of interest. No conflicts have been observed when mapping lineaments of different scales even when the differences were of several orders of magnitude in the same data set.

5. Workflow

The dataset corresponding to the "Residencia Serrana Tanti" (RST) will be used to illustrate the workflow (example files: lines_RST_UTM.shp, DEM_RST_UTM.tif, control_RST_UTM.shp).

MCDA-GIS has been recognized as an important tool in environmental decision makings. In MCDA, the overall objective is to determine a preference ordering among a number of available options (Qashqo, 2018). In GWP-Fracture the main goal is to determine the areas of maximum hydrogeological potential within a hard rock, and the available options are the specific target points into the fracture. There are 4 methods to select these points (figure 2):

- Intersections: consider only those points where two or more fractures intersect.
- Intersections + End Points: considers the intersection points and the extreme points of each trace.
- Intersections + Interval: considers the intersection points and the points defined on the trace at regular intervals.
- Select User Files: considers the intersection points and the points selected by the user.

Once the method has been selected, press the "calculate points" button. Note that intersections have been considered in all available methods because (according to the hydrogeological conceptual model proposed) there is a greater probability of finding water at the intersection of two or more fractures than in an isolated fracture.

After the points have been calculated, the display options and the tabs for line analysis and geomorphometric analysis are enabled (figure 3).

The display options allow you to set a number of output parameters for the maps that will be computed during the following analysis (e.g. point size, line thickness, relief exaggeration, etc.).

The decision–maker's preferences over the options depends on the relative importance of it according to a number of ''criteria'' that have been identified to be the factors on which the decision between options should be made (Eastman, 2012). These criteria are perceived as factors that increase or decrease the suitability of alternatives (e.g., the minimum the slope, the better).

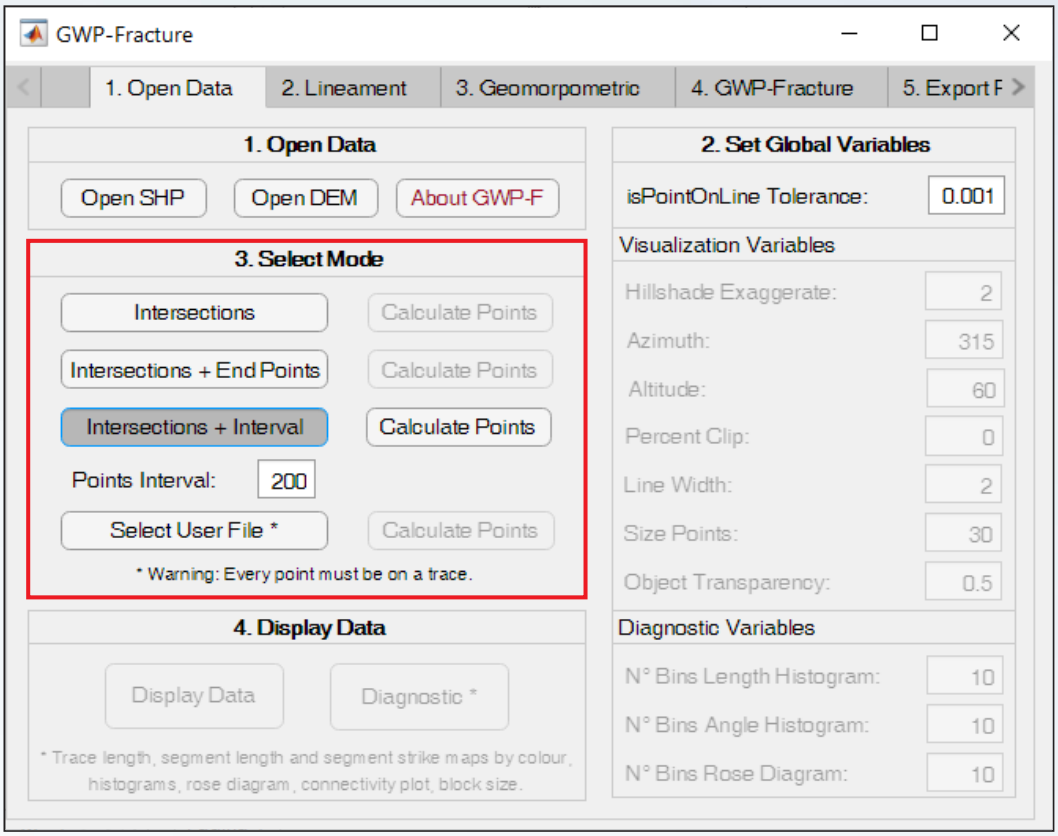

Figure 2: Calculating points.

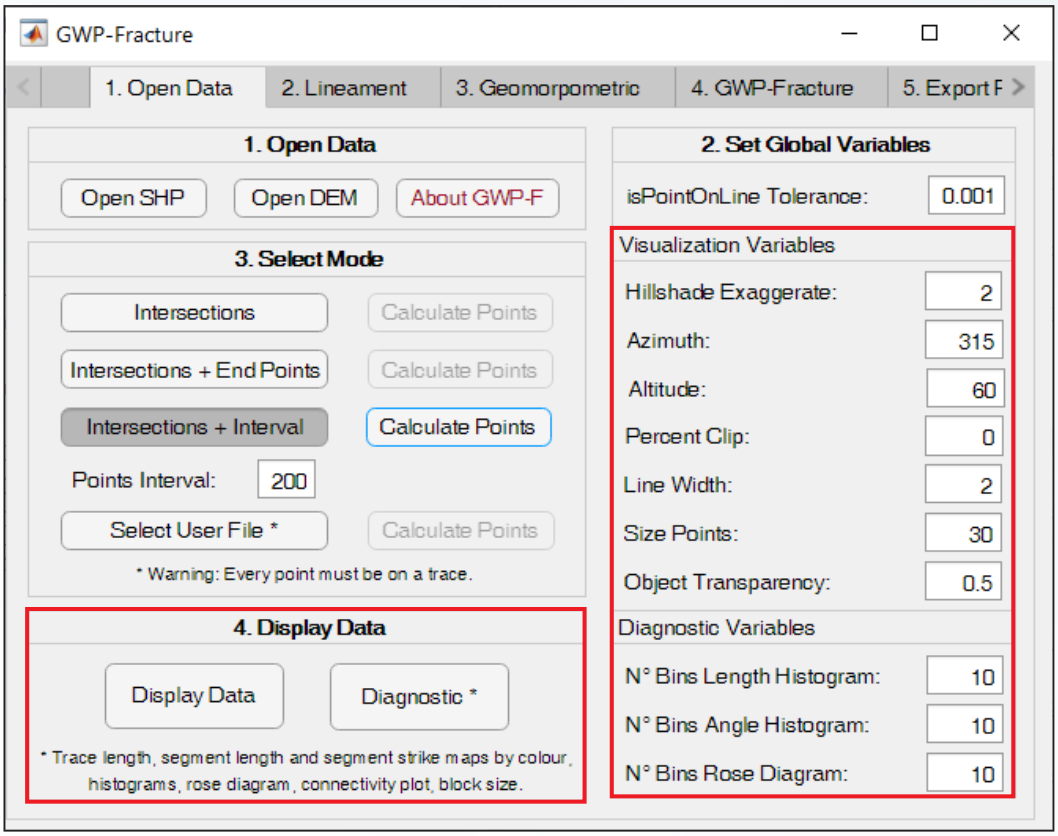

Figure 3: Visualization options

In GWP-Fracture there are two groups of criteria that are analyzed independently. On the one hand, the criteria group related to lineaments mapping (derived from Shape input), called "Lineaments Variables": trace order index (TOI), trace connectivity index (CON), distance to junction's index (DJI) and intensity fracture index (IFI). On the other hand, the criteria related to topography (derived from DEM input), called "Geomorphometric Variables": local slope (SLP), flow accumulation (FACC), topographic wetness index (TWI) and topographic position index-based landforms (TPI). Each of these criteria will be analyzed in greater detail in the following section.

For the criteria analysis (lineaments and geomorphometric), the following steps are sequentially implemented:

1) The scale for the standardization process must be set in the "Normalized Scale os Variables" text box. (figure 4). With this process, since all factors are measured quantitatively, the alternatives are reclassified/ranked order on one common interval scale.

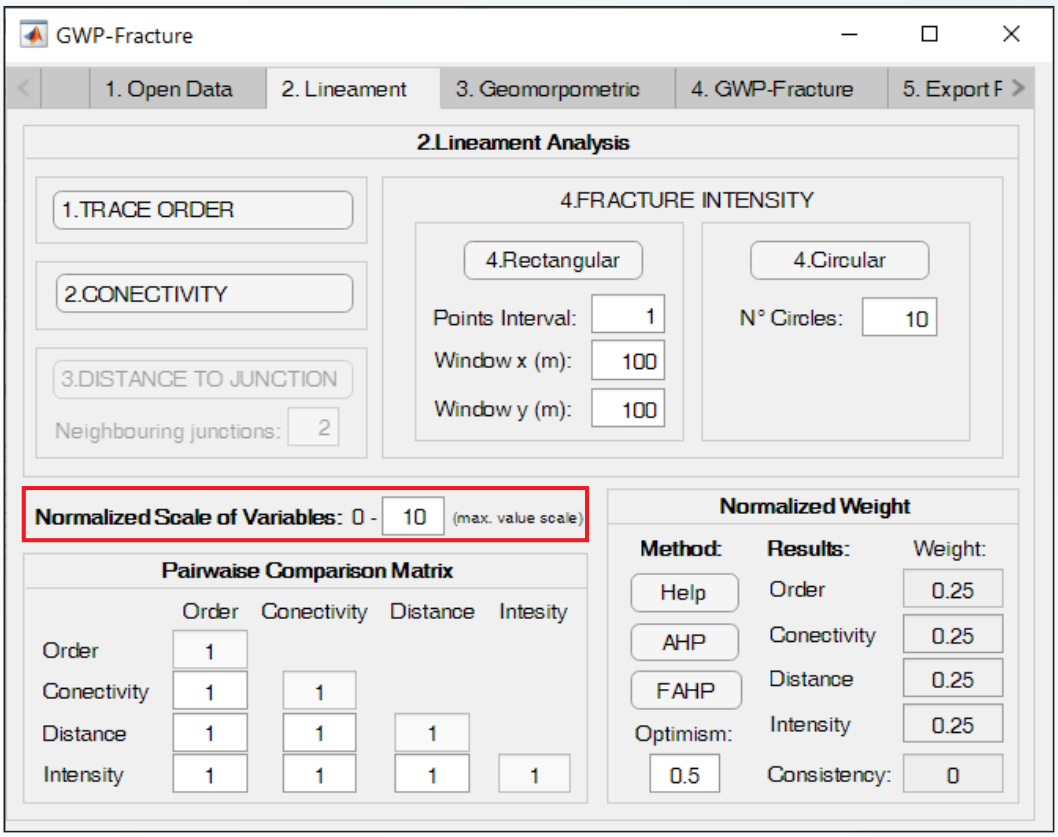

Figure 4: Standardizations process

Two methods are implemented to the standardizations process. The choice of one of them depends on the variable considered. If the range of the variable is known (i.e. SLP and TPI), the standardization process reclassifies the values according to a fixed scale. This fixed scale has been determinate from the literature review.

If the range of the variable is unknown (i.e. TOI, DJI, CON, IFI, FACC and TWI) the standardizations process reclassifies the values according to the equations: $v\_reclas_{(k)} = v_{(k)} * mvs/mvv$ where *v_reclas* is the value of the reclassified variable in the point *k*, *v* is the value of the considered variable in the point *k*, *mvs* is the maximum value of the scale and *mvv* is the maximum value of the observed variable. In this case the standardization process assigns values (in each point) that are proportional to the maximum value found in the range of the considered variable. Thus, the maximum value of the scale is assigned to the maximum value of the considered variable.

2) Suitability maps are derived for each criterion in relation to the main objective To calculate each criterion, just click on the corresponding button (figure 5 y 6).

All criteria must be computed. The input data required for the calculation of each index must be set in its corresponding text box. After the calculation of each criterion, an information box will appear indicating that the task has finished and showing the criteria calculated so far (figure 6). Please wait until the task is finished to continue with the analysis process.

The figure 7 show de obteined results with default parameters.

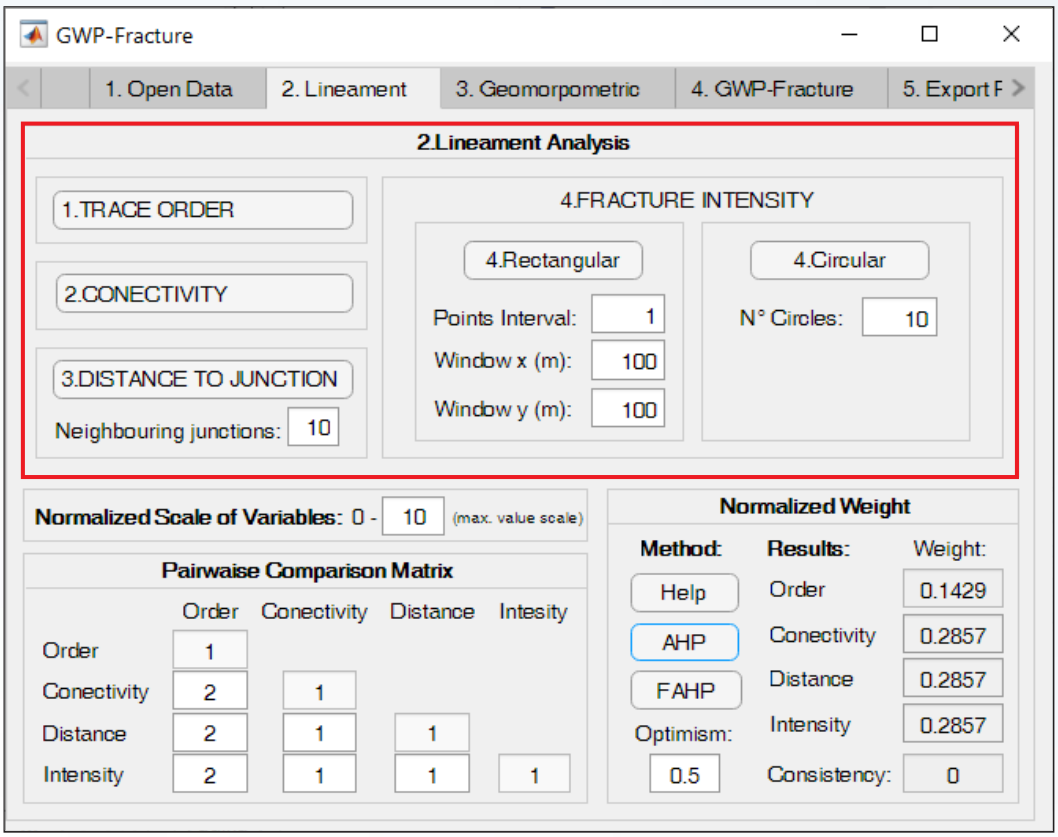

Figure 5: Lineament Analysis.

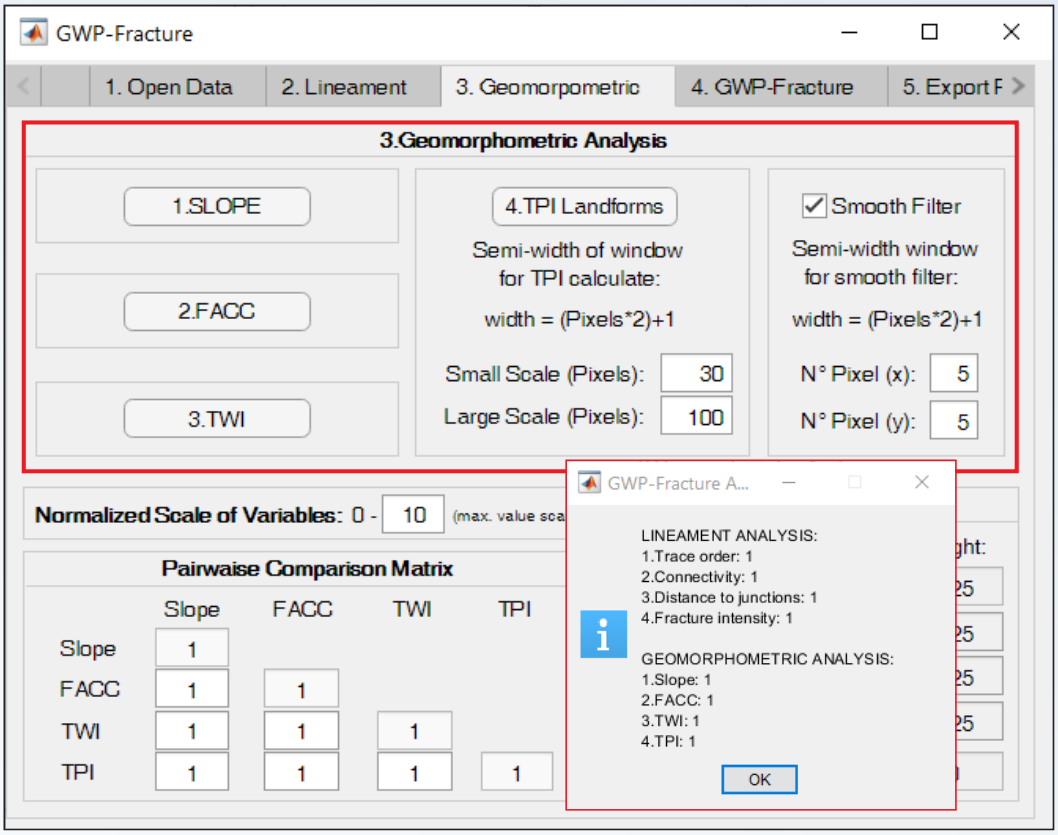

Figure 6: Geomorphometric Analysis.

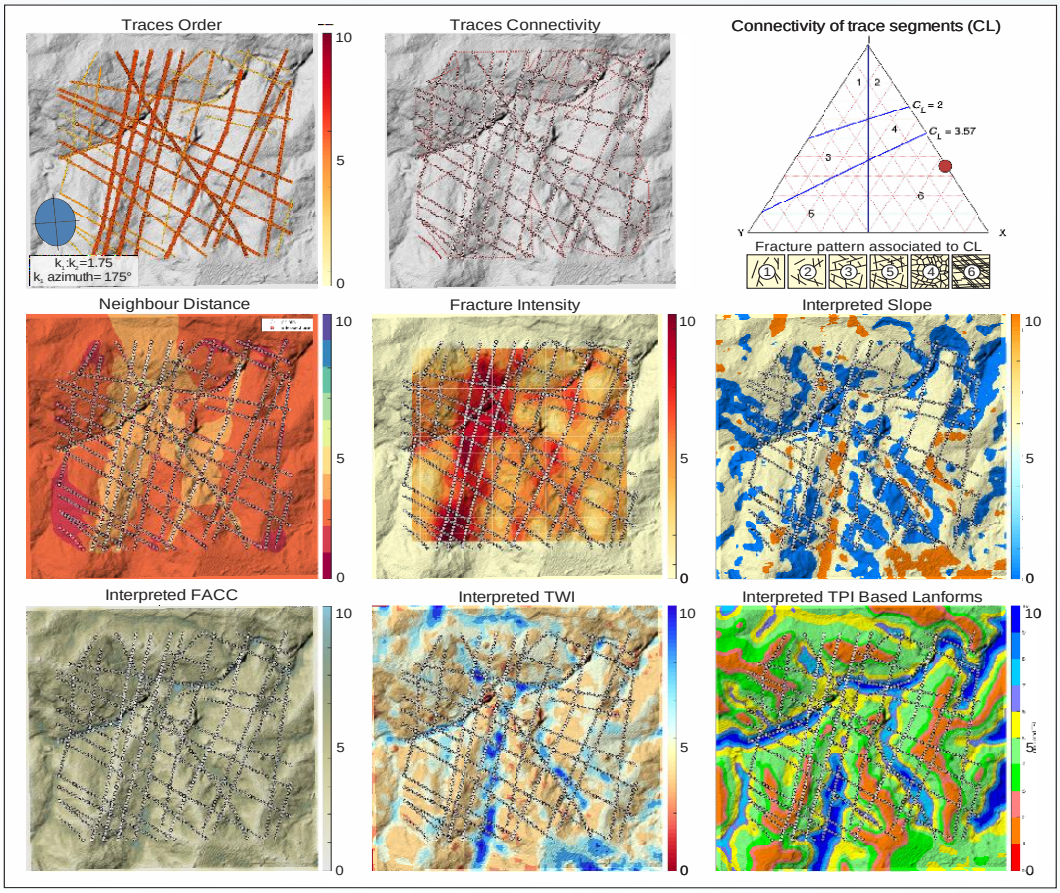

Figure 7: Results obteined.

3) Weights are assigned to the suitability maps in each criteria group. The weights are derived using the analytic hierarchy process (AHP) (Saaty, 1987, 2008, 1990, 1988) or the fuzzy analytic hierarchy process (FAHP) (Chen et al., 2011; Jiang and Eastman, 2000; Wang and Chen, 2008), which are based on pairwise comparisons (figure 8).

AHP uses a ratio scale (table 1), which, contrary to methods using interval scales, requires no units in the comparison. The judgment is a relative value or a quotient a / b of two quantities a and b having the same units (intensity, meters, utility, etc). For help on the basics of the AHP technique and scale values just press the "Help" button (figure 8).

Ranking:	Reciprocal:
9. Extremely strong	1/9. Extremely weak
7. Very strong	1/7. Very weak
5. Strong	1/5. Weak
3. Moderately strong	1/3. Modertely weak
1. Equally strong	
2,4,6,8. Intermediate values between the two adjacent judgments	
1/2,1/4,1/6,1/8. Reciprocal intermediate values	

Table 1: Judgement scale for AHP and FAHP pairwise comparisons.

The results of paired comparisons for n attributes are organized into positive reciprocal n x n matrix S as follows:

$$S = \begin{pmatrix} 1 & \dots & S_{1n} \\ \dots & \dots & \dots \\ 1/S_{1n} & \dots & 1 \end{pmatrix}$$

In addition, the AHP incorporates a useful technique for checking the consistency of the decision maker's evaluations, thus reducing the bias in the decision-making process. The consistency index (*CI*) can be calculated as: $CI = (\lambda_{max} - \mathrm{m})/(m-1)$ where *m* represents the number of independent rows of the matrix and λ_{max} is the highest eigenvalue of the matrix which is calculated as (Saaty, 1977): $\lambda_{\max} = \sum_{j=1}^{m} (S.v)_j / (m.v_j)$. *S* represents pair-wise comparison matrix and *v* means the matrix eigenvector. If the matrix is perfectly consistent then *CI*=0.

When dealing with rising number of pair-wise comparisons the possibility of consistency error is also increasing. Thus, Saaty (1980) suggested the consistency ratio (*CR*) that can be calculated like so: $CR = CI/RI$ where *RI* is represented by average *CI* values gathered from a random simulation of Saaty pair-wise comparison matrices *CIs*. The suggested value of the *CR* should be no higher than 0.1 (Saaty, 1980).

In spite of its popularity, the AHP is often criticized for its inability to incorporate the inherent uncertainty and imprecision associated with mapping the decision-maker's perceptions to exact numbers (Deng, 1999; Vahidnia et al., 2008). Since fuzziness is a common characteristic of decision-making problems, the FAHP method was developed to address this problem (Mikhailov and Tsvetinov, 2004).

FAHP allows decision-makers to express approximate or flexible preferences using fuzzy numbers where adding fuzziness to the input, implies adding fuzziness to the judgment (Chen et al., 2011; Erensal et al., 2006; Feng, 1995; Vahidnia et al., 2009; Wang et al., 2008). GWP-Fracture employs the fuzzy extent analysis proposed by Liou and Wang (1992), which is based on a triangular fuzzy number whose membership function is defined by three real numbers (l, m, u). GWP-Fracture uses a modified version of the code developed by Demet Cilden and Dogus Guler.

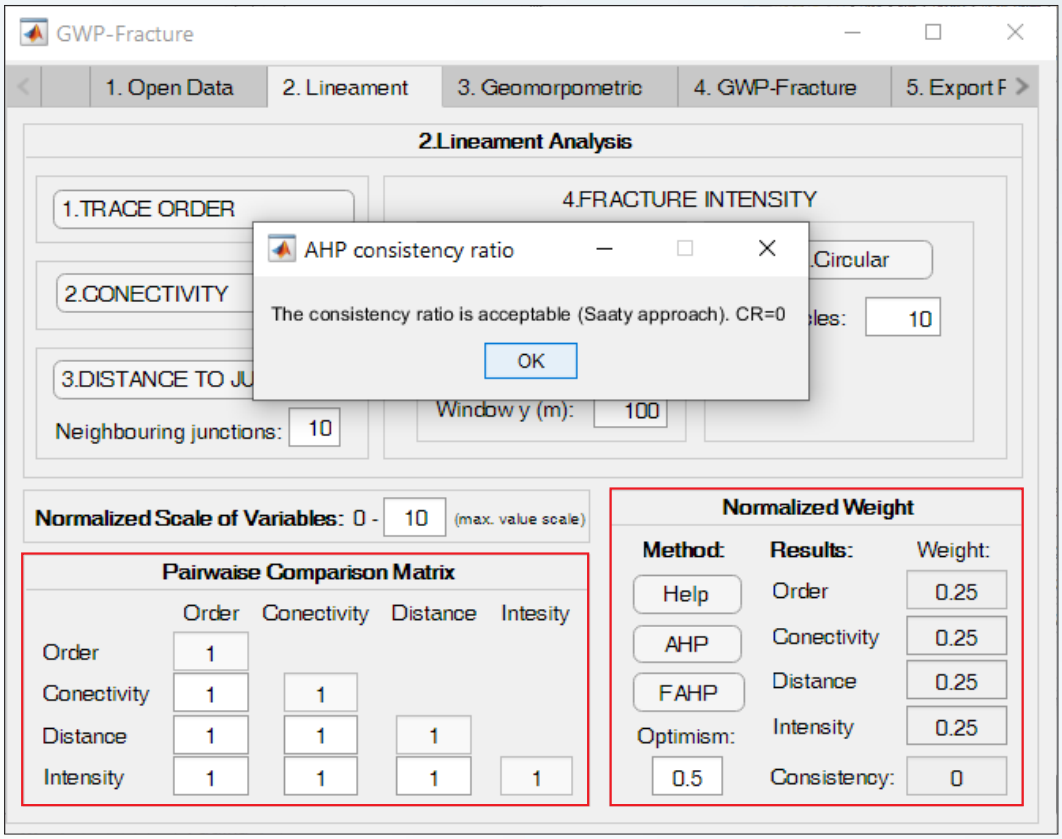

Figure 8: Weighting for each criterion.

3) Finally, a compensatory decision rule is applied, the aim of which is to combine all maps into one single suitability map.

GWP-Fracture use one of the most common additive methods; weighted linear combination (WLC) (CARVER, 1991; Eastman, 1999, 2003). With WLC, the final suitability map is derived by multiplying each factor by its relative weight followed by summation of the results: $S = \sum w_i * x_i$ given w_i as weight of factor i, where $w_i \in [0,1]$ and x_i as the standardized score of factor i where $x_i \in [0, \text{Scale Value}]$ (Eastman, 2012). The groundwater potential index is a dimensionless quantity.

This compensatory decision rule applies twice: Firstly for each criterion within each group of criteria analysed (lineaments and geomorphometrics). In this first WLC, the weights calculated by AHP or FAHP are used. Then, a second decision rule determines the relative weight that each of these groups will have in the final computation of the hydrogeological potential. In this second WLC the weights are determined from the graduated ruler included in the GWP-Fracture tab (figure 9).

The area affected by each fracture (zone of influence) is a function of its length. In the text box "max. fracture influence" the affected area can be set for the longest fracture; the others will be proportional to it.

To compute the GWP-Fracture index just press the "Run GWP-Fracture" button (figure 9).

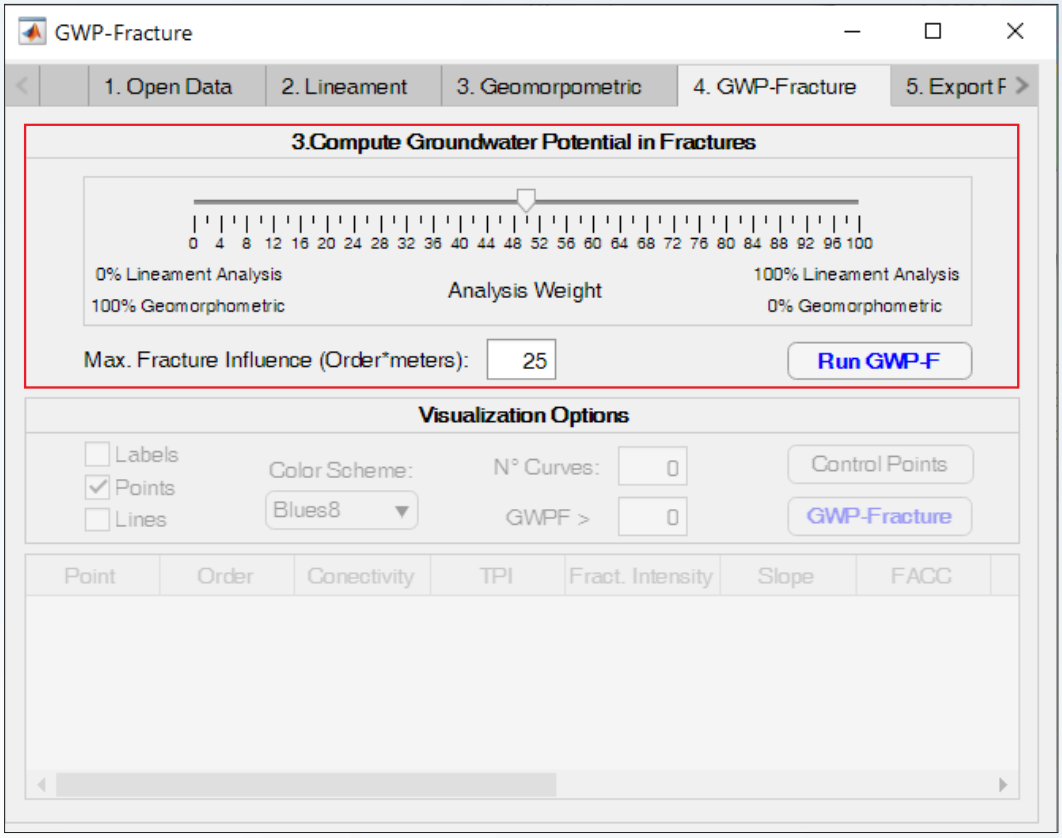

Figure 9: Calculating the groundwater potential.

Once computed, the results for each considered point will be displayed in the built-in table at the bottom of the tab and the display options for groundwater potential delineation maps will be enabled (figure 10).

These options are compatible with and complementary to the options set in the "Open Data" tab, so they can be adjusted from both tabs.

Legends, points and lines can be shown or hidden by clicking on the checkboxes. The color palette can be selected from the "Color Scheme" display button. The text box "GWPF>" allows to limit the range of points shown, only points with an index greater than set are shown. The text box "N°curves" allows to select the number of curves of equal potential that will be drawn.

Finally, the "Control points" button allows you to select a .shp points file to visualize the sites with hydrogeological data. This option allows the maps to be validated, comparing the results obtained with the real data. If the results are not satisfactory, the weights of the variables must be adjusted until an acceptable result is achieved.

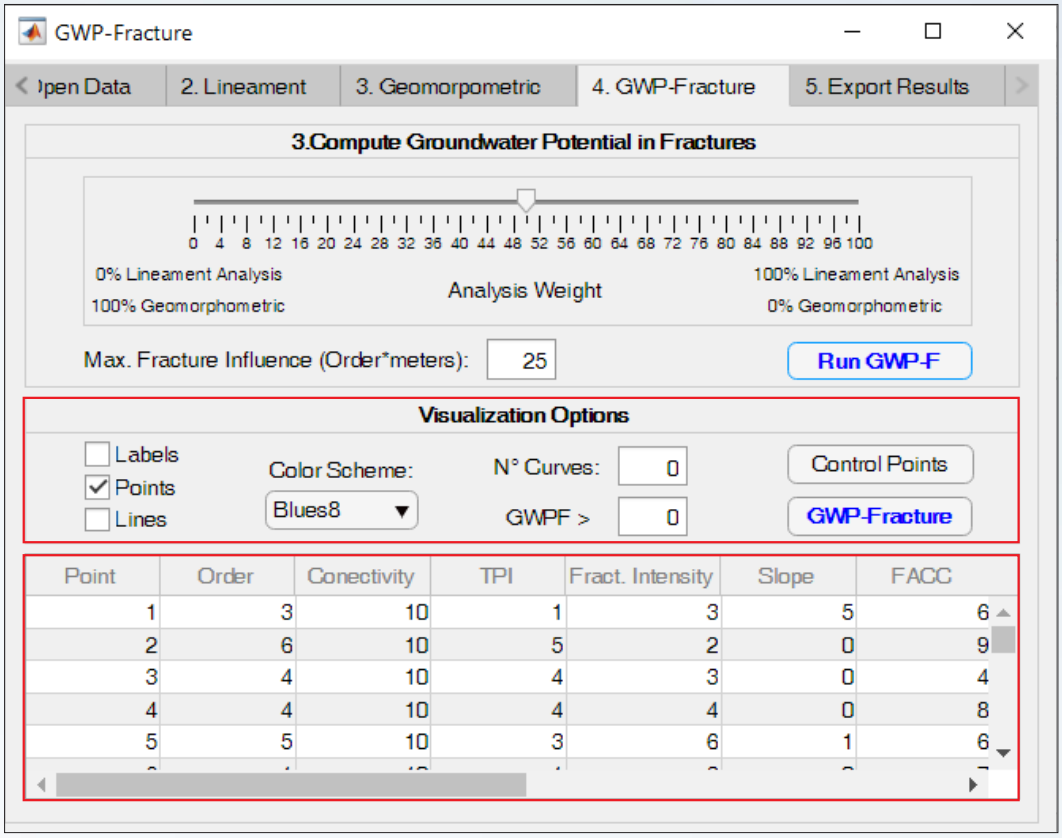

Figure 10: Results table and visualization options for groundwater potential delineation maps.

After selecting the display options and loading the control point data, the "GWP-Fracture" button should be pressed to display the groundwater potential map.

Figure 11 show a summary of the workflow and the steps that are sequentially applied once data has been loaded and target points selected.

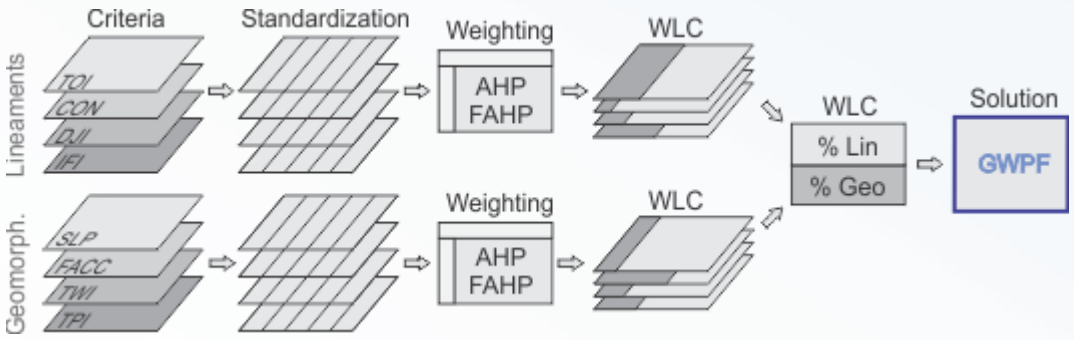

Figure 11: Summary of the workflow in GWP-Fracture.

Figure 12 show the results obtained. The areas with the greatest groundwater potential correspond to the sites where the boreholes have been carried out (black points).

In addition, there is a relationship between the value of the hydrogeological potential and the performance of the wells. Drilling that provides higher flows (in yellow circle, Q>3m³/hs) has been done in sites where the hydrogeological potential acquires the highest values (GWPF index > 70), while low flow drilling (in white circle, Q<1m³/hs) has been made in areas of intermediate potential (GWPF between 50 and 70).

As can be seen, the results obteined can be very useful for preliminary prospecting studies or feasibility studies in areas where there is little or no record of previous hydrogeological studies, allowing to reduce campaign costs to implement more complex prospecting techniques.

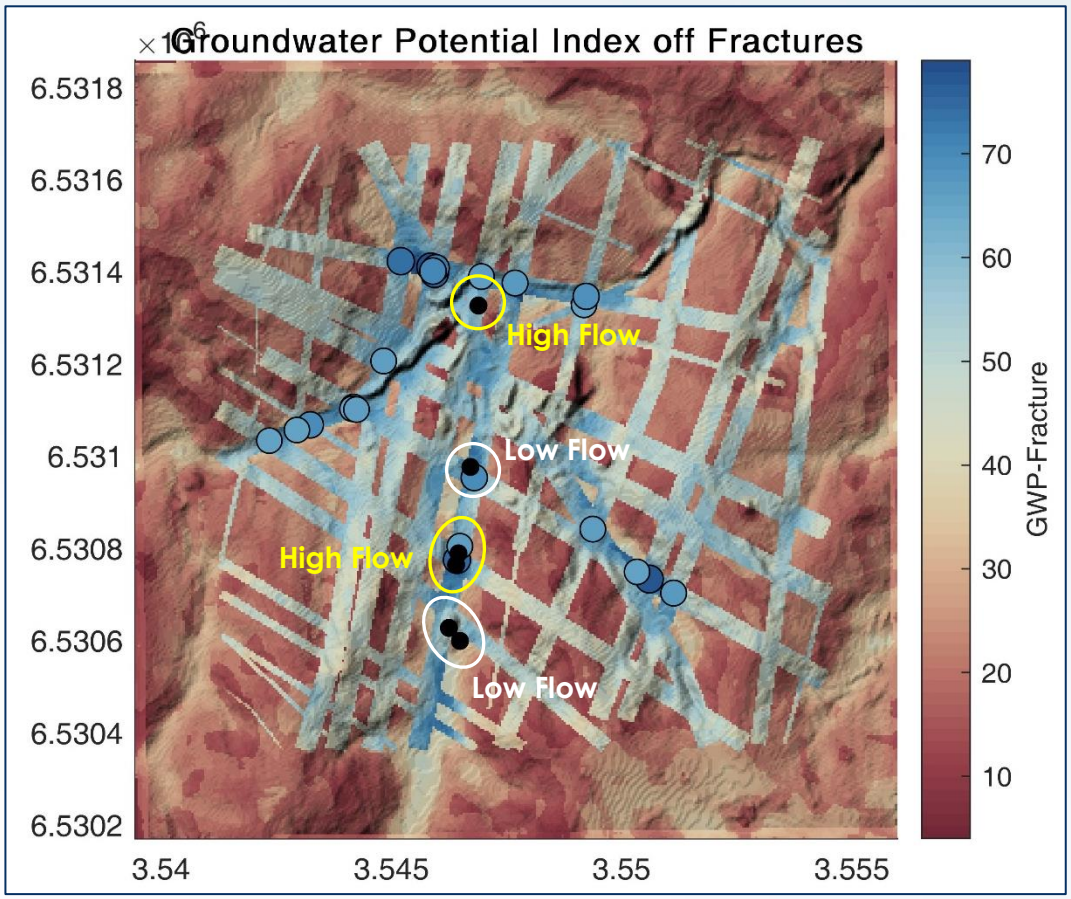

Figure 12: Results obtained and hidrogeological control data.

All results obtained throughout the analysis can be exported in .shp and .tif formats. The export options are presented in the "Export Results" tab (figure 13).

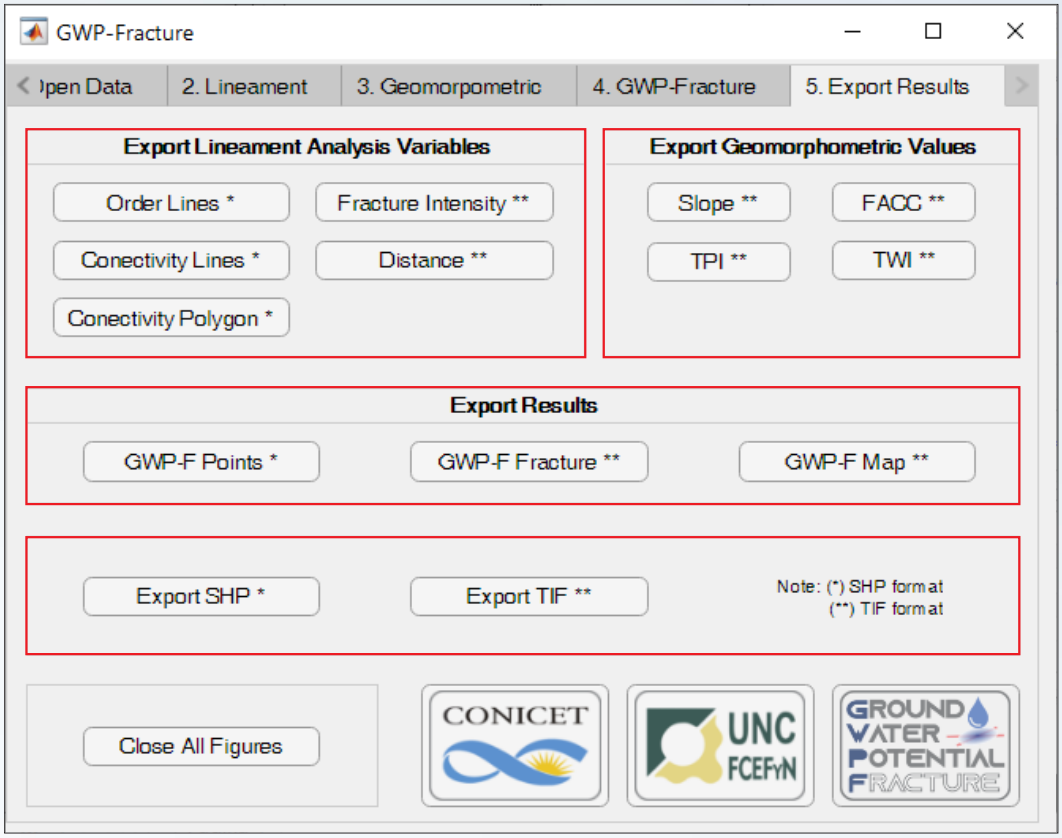

Figure 13: Export options.

6. Criteria Selected

The criteria selection has been made taking into account the principal aspects and categories of thematic layers recognized in the bibliographic research (lineaments, landforms, soil, drainage and geomorphometry).

Two groups of indexes have been selected in order to characterize independently the geological and geomorphological aspects of the hydrogeological environment. These groups are called "Lineament Variables" and "Geomorphometric Variables" respectively.

A total of eight criteria are incorporated in GWP-Fracture. Five of them (IFI, SLP, FACC, TWI and TPI) have been selected from the bibliographic compendium summarized in table 1. The other three criteria have been created with GWP-Frcature (TOI, CON and DJI).

6.1. Lineament variables

Fractures rarely occur in isolation, and their patterns are often highly complex and exert a fundamental influence on the properties of rocks. According to Dershowitz and Einstein (1988) there are two classes of fracture system characterization. Primary characterization concerns those statistics of the system that can be derived by considering each fracture independently. Secondary characterization requires consideration of the system as a whole and concerns spatial correlation between individual fractures within the fracture system.

The quantification of both classes is a necessary precursor to make robust predictions about its extent and scaling in the subsurface (Healy et al., 2017), which ultimately determines the physical properties of the network (i.e. permeability).

In GWP-Fracture primary and secondary characterization are taking into account in the different proposed indexes. According to Gillespie et al. (1993), the full characterization of fracture patterns requires independent analysis of orientation distribution, length distribution, spatial density and connectivity. Orientation and length distribution are contemplating in the Trace Order Index (TOI), spatial density is considered in the Intensity Fracture Index (IFI) and connectivity is evaluated through the Connectivity Index (CON). In addition, Distance to Junctions Index (DJI) analyzes the points proximity to lineament intersections.

6.1.1. Trace Order Index (TOI):

A primary characterization is performed by means of trace length and orientation of each lineament in relation to the 2D permeability tensor's azimuth calculated for the whole fracture system.

Trace length (L) is calculated as the summary of the Euclidean distance between the extreme points of each segment on a trace: $L_{(m)} = \sum_1^n Ls_{(n)}$ where n is the number of segments in the trace m, and Ls is the length for each segment n.

GWP-Fracture make an estimate of permeability in 2D using a modified version of the MATLAB code developed by Healy et al. (2017b) and distributed in the FracPaQ toolbox (guiFracPaQ2Dtensor.m). This code is based on a statistical approach introduced by Oda (1985), to describing and modeling the fluid flow properties of fractured rock (Brown and Bruhn, 1998; Liu et al., 2016; Manzocchi, 2002; Oda, 1985; Oda et al., 1987, 1986; Suzuki et al., 1998). In this approach the permeability properties are related to the fracture geometry through a permeability tensor which is derived by taking a volume average of the expected effect of each fracture in the population. The volume average is calculated through a crack tensor which contains functions of the fracture orientation, length, and aperture in such a way that long fractures or wide fractures contribute relatively more than their smaller cousins.

The crack tensor is calculated as: $P_{ij} = (\pi/4) * \rho * R^2 * T^3 * N_{ij}$ where ρ is the density of fractures (number per unit area), R^2 is the mean of the squared lengths of fractures, T^3 is the mean of the cubed apertures of the fractures and N_{ij} is the orientation matrix (e.g. Woodcock, 1977). Then, following Suzuki et al. (1998), the permeability is: $k_{ij} = (\lambda/12) * (P_{kk} * \delta_{ij} - P_{ij})$ where λ is a factor between 0 and 1, and δ_{ij} is the Kronecker delta. The units of permeability are square meters. kij describes a 2nd order permeability tensor for fluid flow through the fracture network. The ellipse for permeability in the direction of flow, is plotted taking the axes as $\sqrt{k_1}$ and $\sqrt{k_2}$ (see Long et al., 1982).

Note that GWP-Fracture assumes a constant aperture applied to all fractures in the network and a constant coefficient λ. Dealing with aperture variation in the fracture network to include more realistic aperture distributions is a priority for future releases. The factor λ is an empirical constant that can be used to model the degree of connectivity in the fracture network, e.g. a fully connected network has λ=1. Note also that surface roughness and material filling of fractures is not currently considered in the estimate of 2D permeability.

The TOI in the point i is calculated according to: $TOI_{(i)} = \sum_1^j TO_{(j)}$ where j is the number of traces that cross the point i, and TO is the trace order for each trace j.

TO is calculated as: $TO_{(j)} = L_{(j)} * Kf_{(j)}$ where L is the length of the trace j and Kf is a proportional factor of permeability that is calculated according to: $Kf_{(j)} = k_1/k_2 - \left(\left|(\gamma_{(j)} - \alpha)\right| * \frac{(k_1/k_2 - 1)}{90}\right)$. k_1/k_2 is a non-dimensional factor known as permeability ratio (k_1 is the permeability in the maximum permeability direction and k_2 is the permeability in the transverse direction to k_1), γ is the trace angle and a is the 2D permeability tensor's azimuth.

In this sense, longer traces and parallel orientations to the major axis of the ellipse acquires the greatest value of the scale, and the rest of the traces acquires a value that is proportional to their length in relation to the maximum length found.

6.1.2. Trace Connectivity Index (CON):

How fractures are interconnected is critical importance in fractured media. A fractured rock mass can be considered in three dimensions as a volume of rock crossed by a network of fracture planes that, according to their orientations in space, can intercept each other and thus be interconnected.

If only two dimensions are considered, these fracture planes are represented by their traces (line formed by the intersection of the fracture plane and the reference plane considered). The set of individual traces that are connected to each other and isolated from the rest has been called in this work "interconnected entity". In a given reference plane, each interconnected entity represents the minimum expression of the connectivity or interconnection of the fracture network in the three-dimensional space; therefore, defining connectivity in two dimensions is a conservative criterion from the point of view of groundwater prospecting.

CON identifies, compares and classifies each of these interconnected entities by means of the equation: $CON_{(i)} = \mathrm{TL_{(i)}} + \mathrm{A_{(i)}} + \mathrm{NI_{(i)}} + \mathrm{CL_{(i)}}$ where *i* represent the interconnected entity, *TL* is the total length of the traces obtained by adding the length of each individual trace, *A* is the surrounding area of the polygon formed by the nodes corresponding to the ends of these traces, *NI* is the number of intersections within each entity and *CL* is a topological measure (the proportion of nodes I, Y, X) used to describe the relationships between the individual elements that make up each interconnected entity. *CL* is defined from a ternary diagram in which the three vertices of the triangle denote I, Y and X nodes in the fracture network (Manzocchi, 2002; Rohrbaugh et al., 2002a; Sanderson and Nixon, 2015). Nodes are classified as "I" for isolated ends of traces, as "Y" for branch points, splays or abutments, or "X" for cross-cutting intersections. The relative proportions of I, Y and X nodes are calculated with respect to the total number of intersections found, and the connectivity triangle is plotted. More connected networks will plot towards the lower Y-X tie of this diagram, whereas less connected networks will plot towards the I apex. GWP-Fracture also plots two 'contour' lines of connectivity, for C_L = 2.0 and 3.57 where C_L is the number of connections (intersections) per line (or trace), and a 50-50 line for Y-X nodes. According to Sanderson and Nixon (2015), C_L is defined as: $C_L = 4 * (N_Y + N_X)/(N_I + N_Y)$ where N_j refers to the number (not the proportion) of nodes of type j.

6.1.3. Distance to Junctions Index (DJI):

DJI is a measure of the distance between the points considered to evaluate the hydrogeological potential *i* and the points formed by the intersection *j* of two or more traces *k*. The calculation takes into account the average distance from a point to the nearest intersections (DJI). The number of considered intersections *j* is set using the *Neighbouring Junctions* text box. In addition, it takes into account the *Magnitude Order* of intersections according to the TOI calculation. In its mathematical expression the DJI is calculated as: $DJI_{(i)} = d_{min} * d_{scale} * j/\sum_1^j d_{ij} + \sum_1^k TOI_{(k)}/2k$ where d_{min} is the minimum distance founded, d_{scale} is the maximum value of the adopted scale and d_{ij} is the distance between the points *i* and the considered intersections *j*.

In the case where only one neighbor is considered (*j=1*) and (in addition) the point where the index is calculated coincides with an intersection, the distance to the nearest intersection would be 0, since the point of origin and destination would be the same. That value is replaced by a minimum value equal to the pixel size (DEM.cellsize).

If more neighbors are considered (*j>1*), the tendency of the calculation is to increase the value of the index in the direction of the center of gravity of the points considered. It is recommended to adopt a value between *j/10* and *j/20*.

Finally, all point values are interpolated using the standard MATLAB triangulation function to produce the map distribution of DJI.

6.1.4. Fracture Intensity Index (IFI):

Fracture intensity is defined as the total length of fracture in a given area (Dershowitz and Einstein, 1988; Dershowitz and Herda, 1993) and has units of m/m^2. GWP-Fracture provides two methods to compute fracture intensity from the input 2D fracture data:

The first presented method is called "Rectangular". GWP-Fracture generates a 2D grid of evenly spaced rectangular scan windows to fit within the fracture trace map area. Each trace is divided into regular segments from a series of regularly spaced points. The length of these segments and the size of the rectangular scan windows can be adjusted by the user in the text boxes *"Point Interval"* and *"Window (x-y)"* respectively. The code then calculates the numbers of points (and numbers of segments) and the estimated intensity values, for the center of each rectangle, according to: $IFI_{(i)} = (\mathrm{n} - 1) * \mathrm{I}/x * y$ where *n* is the number of points inside an *x* by *y* surface window and *l* is the length defined in the points interval text box. Smaller point intervals will give better results but require longer computation time.

This grid of values is then interpolated using the standard MATLAB triangulation function to produce the maps of estimated rectangular fracture intensity.

The other method, called "Circular", estimates this measure from the data using a modified version of the code developed by Healy et al. (2017b), and distributed in the FracPaQ toolbox (TriScatteredInterp.m). This code is based on the circular scan window method of Mauldon et al. (2001), applied to the coordinate geometry of the fracture trace and segment network. These authors estimated fracture intensity as: $IFI_{(i)} = N/4r$ where N is the number of fractures intersecting the perimeter of a circle of radius r.

GWP-Fracture generates a 2D grid of evenly spaced circular scan windows to fit within the fracture trace map area, where the scan circle diameter is defined as 0.99 of the grids spacing in x and y to avoid overlapping scan circles. The code then calculates the intersections n of the fracture segments within these circles, and calculates the estimated intensity values for the center of each circle. This grid of values is then contoured using the standard MATLAB triangulation function to produce the maps of estimated fracture intensity. The number of circles can be adjusted by the user in the text box "Number of scan circles" (this is the number of scan circles in each of the x- and y-directions, thus the total number of circles is this number squared).

In both presented methods, selecting large numbers (or small size) of scan windows can result in long run-times. The optimum number (or size) of scan windows depends on the specific attributes of the fracture pattern (see Rohrbaugh et al., 2002 for a detailed analysis).

6.2. Geomorphometric variables

Based on the literature review summarized in table 1, four geomorphometric indexes were selected in GWP-Fracture: slope angle (SLP), flow accumulation (FACC), topographic wetness index (TWI), and topographic position index based-landform (TPI).

SLP and FACC are important factors to quantify the infiltration processes and drainage characteristics. TWI is an indicator of soil moisture content. Finally, TPI is a simple and repeatable method to classify the landscape into slope position and landform category.

6.2.1. Slope (SLP):

The *slope* (or *gradient*) is a measure of the steepness, the incline or the grade of a surface measured in either percentages or degrees (H. Trauth, 2015). Slope is a significant factor for the detection of groundwater prospective zones (Ghosh et al., 2016). Steeper slopes cause less recharge because of rapid runoff during rainfall, allowing insufficient time to infiltrate the surface and recharge the saturated zone (Gumma and Pavelic, 2013; Magesh et al., 2012; Rokade et al., 2007; Selvam et al., 2014).

The *slope* of a DEM cell may be differently defined. In GWP-Fracture the trigonometrical maximum downward gradient is taken (Warren et al., 2004). Finding the maximum gradient requires the calculation of all slopes between all neighboring cells. The slope S_{ij} between two neighbor cells i and j is calculated by: $S_{ij} = (z_i - z_j)/d_{ij}$ where d_{ij} is the distance between the cells i and j, and z is the elevation.

6.2.2. Flow Accumulation (FACC):

Flow accumulation (FACC), also called specific catchment area, is defined as the number of cells (or area) contributing runoff to a particular cell (H. Trauth, 2015). Its calculation is based on the information of flow direction (FD) (Wilson and Gallant, 2000). By counting the number of cells draining in each grid cell, FACC algorithms calculate the upslope contributing drainage area which serves as measure for discharge in many modelling approaches.

GWP-Fracture calculate FACC and FD from modified versions of the codes developed by Schwanghart and Kuhn (2010) and distributed in the TopoToolbox toolbox (flowacc.m and FlowObj.m).

Flow direction determines the surficial movement of water through terrain. Various algorithms have been proposed to determine flow directions (e.g. Orlandini et al., 2003; Qin et al., 2007; Qin and Zhan, 2012; Seibert and McGlynn, 2007; Tarboton, 1997; Wolock and McCabe, 1995; Zhang et al., 2017). According to Schwanghart and Kuhn (2010), FD can be represented within the transfer matrix (M). Elements in M contain the relative amount of discharge M_{ij} transferred from one cell i to a maximum number of eight downward neighbors with the index j. Thereby the transfer ratios are proportional to the downward slope to the respective neighbor: $M_{ij} \sim max\{S_{ij}, 0\}$.

The authors derive the upslope area from the flow direction matrix M using a set of coupled equations. They derive the linear system from the equilibrium equations of network flow without capacity constraints with the flow rates as unknowns (see Schwanghart and Kuhn, 2010 for a detailed analysis). In this way, FACC can be determined as the steady state flow rate in each cell during a constant inflow to each cell of 1 unit per time unit. In matrix notation the implemented equation is: $w = (I - M^T)^{-1} f0$ where I is the identity matrix and M^T is the transpose of the flow direction matrix outlined above. w is a $n \times 1$ vector containing the storage values in each cell and $f0$ is a $n \times 1$ vector where the values correspond to the inflow rates in each cell.

6.2.3. Topographic Wetness Index (TWI):

TWI is an important topographic index which can quantify the effect of topography on runoff generation and serves as a physically-based index approximating the location of zones of surface saturation and the spatial distribution of soil water (Barling et al., 1994; BEVEN and KIRKBY, 1979; O'Loughlin, 1986; Qin et al., 2011).

The TWI for a cell i is the log of the ratio between the area of the catchment for that particular cell (FACC) and the tangent of its slope (SLP) (H. Trauth, 2015): $TWI_{(i)} = log\left(1 + FACC_{(i)}\right)/tan\left(SLP_{(i)}\right)$. The term 1+*FACC* avoids the problems associated with calculating the logarithm of zero when *FACC=0*.

The TWI is used to predict the soil water content (saturation) resulting from lateral water movement. The potential for waterlogging is usually highest in the lower parts of catchments, where the slopes are gentler. Flat areas with a large upslope area have a high wetness index compared to steep areas with small catchments.

6.2.4. Topographic Position Index Based Landforms Classifications (TPI):

In geomorphological context, a landform may give a clue to surface and subsurface water conditions (Nagarale, 2017). The TPI provides a concise and effective method of landscape classification in accordance with morphology (Weiss, 2001).

Its fundamental principle is to compare the elevation of each cell in a DEM to the mean elevation of a specified neighborhood around that cell.

Positive TPI values represent locations that are higher than the average of their surroundings (ridges). Negative TPI values represent locations that are lower than their surroundings (valleys). TPI values near zero are either flat areas (where the slope is near zero) or areas of constant slope (where the slope of the point is significantly greater than zero). This rule is presented by: $TPI_{(radius)} = (E - E_{mean})/E_{max}$ where $radius$ means the distance of the neighborhood, E signifies the current elevation, E_{mean} represents the mean elevation of the neighborhood, and E_{max} denotes the maximum elevation.

By thresholding the continuous TPI values at a given scale, and checking the slope for values near zero, landscapes can be classified into discrete slope position classes (Weiss, 2001). One repeatable method of creating classes, is to use standard deviation units. The TPI slope can be computed by the elevation difference between the neighbor pixels and the slope. The choice of the neighborhood scale will influence the result of the TPI slope classification.

To eliminate the impact of the neighborhood range on the TPI slope, small TPI and large TPI radius are used (Weiss, 2001). They are calculated by relatively small and large neighborhood ranges, together with the topographic slope, and then combined in different classes. As a general rule, because elevation tends to be spatially autocorrelated, the range of TPI values increases with scale. One method to address this problem is to standardize the TPI grids to mean = 0 and stdev = 1. This lets the same basic equations to be used to classify any scale combinations of TPI grids. Then, a new set of parameters—TPI landform position classes is acquired. Landforms are then classified using TPI grid thresholds (Table 2).

Class	Landforms	Neighborhood TPI		Slope	Interpreted GWP
		Small TPI	Large TPI		
1	Lowland, small depressions	≤ -1	≤ -1		10
2	Upper flat dells, flat sinks	≤ -1	> -1 and < 1		9
3	Flat hollows in culmination areas	≤ -1	≥ 1		8
4	Lowland, larger depressions	> -1 and < 1	≤ -1		7
5	Flat relief, plains ≤ 2°	> -1 and < 1	> -1 and < 1	≤ 2°	6
6	Slope > 2°	> -1 and < 1	> -1 and < 1	> 2°	5
7	Culimnation area	> -1 and < 1	≥ 1		4
8	Local elevation in lowlands	≥ 1	≤ -1		3
9	Mid-slope small ridges	≥ 1	> -1 and < 1		2
10	Top, shoulder	≥ 1	≥ 1		1

Table 2: TPI grid thresholds (Weiss, 2001).

7. Scope for further improvements

In addition to removing any bugs and improve the run-time of the computationally heavier processing tasks (e.g. calculating points and traces to be used, calculating fracture intensity using the scan line method, calculating connectivity, etc.), it is also intended to implement improvements and extensions in future releases of the code. These currently include:

Incorporate an automatic adjustment method for the weights of each variable based on correlations with in situ observed hydrogeological data (e.g. flow rate) and the estimated groundwater potential obtained.

Achieve better estimates of 2D permeability based on observed inputs as aperture distributions, roughness, and filling, rather than assuming a constant permeability, or coupling permeability to length (Gudmundsson et al., 2001; Vermilye and Scholz, 1995).

Contemplate different depths for the analysis of the lineament's variables. The possibility of projecting the traces on a reference plane to a specific depth is considered. In order to do this, it is necessary to incorporate the dip of each of the discontinuities as an input data. The closure of the traces aperture with depth can be estimated as a function of its order of magnitude.

Incorporate more geomorphometric indices such as multi-resolution valley-bottom flatness (MVRFB) (Gallant and Dowling, 2003), Stream Power Index (SPI) (Moore et al., 1991), LS Factor (Kinnell, 2005), etc.

Allow the user to incorporate additional layers of his own for the calculation of the groundwater potential (e.g. lithology, land use, precipitation, etc.), not only within the fractures but also in their surroundings (within the intact rock massif).

8. References

Analytic Hierarchy Process (AHP) for Examining Healthcare Professionals' Assessments of Risk Factors,.

Barling, R.D., Moore, I.D., Grayson, R.B., 1994. A quasi-dynamic wetness index for characterizing the spatial distribution of zones of surface saturation and soil water content. Water Resour. Res. 30, 1029–1044. https://doi.org/10.1029/93WR03346

Barrocu, G., 2007. Hydrogeology of granite rocks in Sardinia, in: Krásny, J., Sharp, J.M. (Eds.), Groundwater in Fractured Rocks: Selected Papers from the Groundwater in Fractured Rocks International Conference, Prague, 2003. Taylor & Francis, The Netherlands, pp. 33–44. https://doi.org/10.1201/9780203945650.pt1

BEVEN, K.J., KIRKBY, M.J., 1979. A physically based, variable contributing area model of basin hydrology / Un modèle à base physique de zone d'appel variable de l'hydrologie du bassin versant. Hydrol. Sci. Bull. 24, 43–69. https://doi.org/10.1080/02626667909491834

Brown, S.R., Bruhn, R.L., 1998. Fluid permeability of deformable fracture networks. J. Geophys. Res. Solid Earth 103, 2489–2500. https://doi.org/10.1029/97jb03113

CARVER, S.J., 1991. Integrating multi-criteria evaluation with geographical information systems. Int. J. Geogr. Inf. Syst. 5, 321–339. https://doi.org/10.1080/02693799108927858

Chandra, S., Auken, E., Maurya, P.K., Ahmed, S., Verma, S.K., 2019. Large Scale Mapping of Fractures and Groundwater Pathways in Crystalline Hardrock By AEM. Sci. Rep. 9, 1–11. https://doi.org/10.1038/s41598-018-36153-1

Chen, Y.-H., Wang, T.-C., Wu, C.-Y., 2011. Multi-criteria decision making with fuzzy linguistic preference relations. Appl. Math. Model. 35, 1322–1330. https://doi.org/10.1016/j.apm.2010.09.009

Deng, H., 1999. Multicriteria analysis with fuzzy pairwise comparison. Int. J. Approx. Reason. 21, 215–231. https://doi.org/10.1016/S0888-613X(99)00025-0

Dershowitz, W.S., Einstein, H.H., 1988. Characterizing rock joint geometry with joint system models. Rock Mech. Rock Eng. 21, 21–51. https://doi.org/10.1007/BF01019674

Dershowitz, W.S., Herda, H.H., 1993. Interpretation of fracture spacing and intensity. Int. J. Rock Mech. Min. Sci. Geomech. Abstr. 30, 212. https://doi.org/10.1016/0148-9062(93)91769-F

Eastman, J., 1999. Multi-criteria evaluation and GIS. Geogr. Inf. Syst. 1, 493-502.

Eastman, J.R., 2012. IDRISI Selva Manual. IDRISI Selva Man. https://doi.org/10.1109/TGRS.2002.802519

Eastman, J.R., 2003. IDRISI Kilimanjaro: Guide to GIS and Image Processing. Clark Univ. Worcester, MA, USA 1, 87–131. https://doi.org/10.1109/TGRS.2002.802519

Erensal, Y.C., Öncan, T., Demircan, M.L., 2006. Determining key capabilities in technology management using fuzzy analytic hierarchy process: A case study of Turkey. Inf. Sci. (Ny). 176, 2755–2770. https://doi.org/10.1016/j.ins.2005.11.004

Feng, C., 1995. Fuzzy multicriteria decision-making in distribution of factories: an application of approximate reasoning. Fuzzy Sets Syst. 71, 197–205. https://doi.org/10.1016/0165-0114(94)00238-3

Gallant, J.C., Dowling, T.I., 2003. A multiresolution index of valley bottom flatness for mapping depositional areas. Water Resour. Res. 39. https://doi.org/10.1029/2002WR001426

Ghosh, P.K., Bandyopadhyay, S., Jana, N.C., 2016. Mapping of groundwater potential zones in hard rock terrain using geoinformatics: a case of Kumari watershed in western part of West Bengal. Model. Earth Syst. Environ. 2, 12. https://doi.org/10.1007/s40808-015-0044-z

Gillespie, P.A., Howard, C.B., Walsh, J.J., Watterson, J., 1993. Measurement and characterisation of spatial distributions of fractures. Tectonophysics 226, 113–141. https://doi.org/10.1016/0040-1951(93)90114-Y

Gudmundsson, A., Berg, S.S., Lyslo, K.B., Skurtveit, E., 2001. Fracture networks and fluid transport in active fault zones. J. Struct. Geol. 23, 343–353. https://doi.org/10.1016/S0191-8141(00)00100-0

Gumma, M.K., Pavelic, P., 2013. Mapping of groundwater potential zones across Ghana using remote sensing, geographic information systems, and spatial modeling. Environ. Monit. Assess. 185, 3561–3579. https://doi.org/10.1007/s10661-012-2810-y

Gustafsson, P., 1994. Spot Satellite Data For Exploration Of Fractured Aquifers In A Semi-Arid Area In Southeastern Botswana. Hydrogeol. J. 2, 9–18. https://doi.org/10.1007/s100400050246

H. Trauth, M., 2015. MATLAB® Recipes for Earth Sciences, MATLAB Recipes for Earth Sciences, Fourth Edition. Springer Berlin Heidelberg, Berlin, Heidelberg. https://doi.org/10.1007/978-3-662-46244-7

Healy, D., Rizzo, R.E., Cornwell, D.G., Farrell, N.J.C., Watkins, H., Timms, N.E., Gomez-Rivas, E., Smith, M., 2017. FracPaQ: A MATLAB™ toolbox for the quantification of fracture patterns. J. Struct. Geol. 95, 1–16. https://doi.org/10.1016/j.jsg.2016.12.003

Jafari, A., Babadagli, T., 2011. Effective fracture network permeability of geothermal reservoirs. Geothermics 40, 25–38. https://doi.org/10.1016/j.geothermics.2010.10.003

Jafari, A., Babadagli, T., 2009. A Sensitivity Analysis for Effective Parameters on 2D Fracture-Network Permeability. SPE Reserv. Eval. Eng. 12, 455–469. https://doi.org/10.2118/113618-PA

Jiang, H., Eastman, J.R., 2000. Application of fuzzy measures in multi-criteria evaluation in GIS. Int. J. Geogr. Inf. Sci. 14, 173–184. https://doi.org/10.1080/136588100240903

Kinnell, P.I.A., 2005. ALTERNATIVE APPROACHES FOR DETERMINING THE USLE-M SLOPE LENGTH FACTOR FOR GRID CELLS. Soil Sci. Soc. Am. J. 69, 674. https://doi.org/10.2136/sssaj2004.0047

Liou, T.-S., Wang, M.-J.J., 1992. Ranking fuzzy numbers with integral value. Fuzzy Sets Syst. 50, 247–255. https://doi.org/10.1016/0165-0114(92)90223-Q

Liu, R., Li, B., Jiang, Y., Huang, N., 2016. Review: Mathematical expressions for estimating equivalent permeability of rock fracture networks. Hydrogeol. J. 24, 1623–1649. https://doi.org/10.1007/s10040-016-1441-8

Long, J.C.S., Remer, J.S., Wilson, C.R., Witherspoon, P.A., 1982. Porous media equivalents for networks of discontinuous fractures. Water Resour. Res. 18, 645–658. https://doi.org/10.1029/WR018i003p00645

Magesh, N.S., Chandrasekar, N., Soundranayagam, J.P., 2012. Delineation of groundwater potential zones in Theni district, Tamil Nadu, using remote sensing, GIS and MIF techniques. Geosci. Front. 3, 189–196. https://doi.org/10.1016/j.gsf.2011.10.007

Manzocchi, T., 2002. The connectivity of two-dimensional networks of spatially correlated fractures. Water Resour. Res. 38, 1-1-1–20. https://doi.org/10.1029/2000WR000180

Mauldon, M., Dunne, W.M., Rohrbaugh, M.B., 2001. Circular scanlines and circular windows: new tools for characterizing the geometry of fracture traces. J. Struct. Geol. 23, 247–258. https://doi.org/10.1016/S0191-8141(00)00094-8

Mikhailov, L., Tsvetinov, P., 2004. Evaluation of services using a fuzzy analytic hierarchy process. Appl. Soft Comput. 5, 23–33. https://doi.org/10.1016/j.asoc.2004.04.001

Moore, I.D., Grayson, R.B., Ladson, A.R., 1991. Digital terrain modelling: A review of hydrological, geomorphological, and biological applications. Hydrol. Process. 5, 3–30. https://doi.org/10.1002/hyp.3360050103

Nagarale, V.R., 2017. Geography Groundwater Zonation by using Landform Characteristics in Karha River Basin , Pune. S.N.D.T. Women's University Pune Campus.

O'Loughlin, E.M., 1986. Prediction of Surface Saturation Zones in Natural Catchments by Topographic Analysis. Water Resour. Res. 22, 794–804. https://doi.org/10.1029/WR022i005p00794

Oda, M., 1985. Permeability tensor for discontinuous rock masses. Géotechnique 35, 483–495. https://doi.org/10.1680/geot.1985.35.4.483

Oda, M., Hatsuyama, Y., Ohnishi, Y., 1987. Numerical experiments on permeability tensor and its application to jointed granite at Stripa Mine, Sweden. J. Geophys. Res. 92, 8037. https://doi.org/10.1029/JB092iB08p08037

Oda, M., Yamabe, T., Kamemura, K., 1986. A crack tensor and its relation to wave velocity anisotropy in jointed rock masses. Int. J. Rock Mech. Min. Sci. 23, 387–397. https://doi.org/10.1016/0148-9062(86)92304-1

Orlandini, S., Moretti, G., Franchini, M., Aldighieri, B., Testa, B., 2003. Path-based methods for the determination of nondispersive drainage directions in grid-based digital elevation models. Water Resour. Res. 39. https://doi.org/10.1029/2002WR001639

Qashqo, B., 2018. GIS-Based Multi-Criteria Decision Analysis for identifying water distribution points: a case study in Lapilang & Suspa regions, Nepal. University of Salzburg, Austria.

Qin, C.-Z., Zhan, L., 2012. Parallelizing flow-accumulation calculations on graphics processing units—From iterative DEM preprocessing algorithm to recursive multiple-flow-direction algorithm. Comput. Geosci. 43, 7–16. https://doi.org/10.1016/j.cageo.2012.02.022

Qin, C.-Z., Zhu, A.-X., Pei, T., Li, B.-L., Scholten, T., Behrens, T., Zhou, C.-H., 2011. An approach to computing topographic wetness index based on maximum downslope gradient. Precis. Agric. 12, 32–43. https://doi.org/10.1007/s11119-009-9152-y

Qin, C., Zhu, A. -X., Pei, T., Li, B., Zhou, C., Yang, L., 2007. An adaptive approach to selecting a flow-partition exponent for a multiple-flow-direction algorithm. Int. J. Geogr. Inf. Sci. 21, 443–458. https://doi.org/10.1080/13658810601073240

Rohrbaugh, J.B., Dunne, W.M., Mauldon, M., 2002a. Estimating fracture trace intensity, density, and mean length using circular scan lines and windows. Am. Assoc. Pet. Geol. Bull. 86, 2089–2104. https://doi.org/10.1306/61EEDE0E-173E-11D7-8645000102C1865D

Rohrbaugh, J.B., Dunne, W.M., Mauldon, M., 2002b. Estimating fracture trace intensity, density, and mean length using circular scan lines and windows. Am. Assoc. Pet. Geol. Bull. 86, 2089–2104. https://doi.org/10.1306/61EEDE0E-173E-11D7-8645000102C1865D

Rokade, V.M., Kundal, P., Joshi, A.K., 2007. Groundwater potential modelling through remote sensing and GIS: A case study from Rajura Taluka, Chandrapur District, Maharashtra. J. Geol. Soc. India 69, 943–948.

Saaty, R.W., 1987. The analytic hierarchy process—what it is and how it is used. Math. Model. 9, 161–176. https://doi.org/10.1016/0270-0255(87)90473-8

Saaty, T.L., 2008. Decision making with the analytic hierarchy process. Int. J. Serv. Sci. 1, 83. https://doi.org/10.1504/IJSSCI.2008.017590

Saaty, T.L., 1990. How to make a decision: The analytic hierarchy process. Eur. J. Oper. Res. 48, 9–26. https://doi.org/10.1016/0377-2217(90)90057-I

Saaty, T.L., 1988. What is the Analytic Hierarchy Process?, in: Mathematical Models for Decision Support. Springer Berlin Heidelberg, Berlin, Heidelberg, pp. 109–121. https://doi.org/10.1007/978-3-642-83555-1_5

Saaty, T.L., 1980. The Analytic Hierarchy Process, Decision Analysis. https://doi.org/10.3414/ME10-01-0028

Saaty, T.L., 1977. A scaling method for priorities in hierarchical structures. J. Math. Psychol. 15, 234–281. https://doi.org/10.1016/0022-2496(77)90033-5

Sanderson, D.J., Nixon, C.W., 2015a. The use of topology in fracture network characterization. J. Struct. Geol. 72, 55–66. https://doi.org/10.1016/j.jsg.2015.01.005

Sanderson, D.J., Nixon, C.W., 2015b. The use of topology in fracture network characterization. J. Struct. Geol. 72, 55–66. https://doi.org/10.1016/j.jsg.2015.01.005

Schneeberger, R., Egli, D., Lanyon, G.W., Mäder, U.K., Berger, A., Kober, F., Herwegh, M., 2018. Structural-permeability favorability in crystalline rocks and implications for groundwater flow paths: a case study from the Aar Massif (central Switzerland). Hydrogeol. J. 26, 2725–2738. https://doi.org/10.1007/s10040-018-1826-y

Schwanghart, W., Kuhn, N.J., 2010. TopoToolbox: A set of Matlab functions for topographic analysis. Environ. Model. Softw. 25, 770–781. https://doi.org/10.1016/j.envsoft.2009.12.002

Seibert, J., McGlynn, B.L., 2007. A new triangular multiple flow direction algorithm for computing upslope areas from gridded digital elevation models. Water Resour. Res. 43. https://doi.org/10.1029/2006WR005128

Selvam, S., Magesh, N.S., Sivasubramanian, P., Soundranayagam, J.P., Manimaran, G., Seshunarayana, T., 2014. Deciphering of groundwater potential zones in Tuticorin, Tamil Nadu, using remote sensing and GIS techniques. J. Geol. Soc. India 84, 597–608. https://doi.org/10.1007/s12594-014-0167-2

Sharp, J.M. (Ed.), 2014. Fractured Rock Hydrogeology, Fractured Rock Hydrogeology. CRC Press. https://doi.org/10.1201/b17016

Suzuki, K., Oda, M., Yamazaki, M., Kuwahara, T., 1998. Permeability changes in granite with crack growth during immersion in hot water. Int. J. Rock Mech. Min. Sci. 35, 907–921. https://doi.org/10.1016/S0148-9062(98)00016-3

Tarboton, D.G., 1997. A new method for the determination of flow directions and upslope areas in grid digital elevation models. Water Resour. Res. 33, 309–319. https://doi.org/10.1029/96WR03137

Vahidnia, M.H., Alesheikh, A., Alimohammadi, A., Bassiri, A., 2008. Fuzzy analytical hierarchy process in GIS application. Int. Arch. Photogramm. Remote Sens. Spat. Inf. Sci. 37, 593–596.

Vahidnia, M.H., Alesheikh, A.A., Alimohammadi, A., 2009. Hospital site selection using fuzzy AHP and its derivatives. J. Environ. Manage. 90, 3048–3056. https://doi.org/10.1016/j.jenvman.2009.04.010

Vermilye, J.M., Scholz, C.H., 1995. Relation between vein length and aperture. J. Struct. Geol. 17, 423–434. https://doi.org/10.1016/0191-8141(94)00058-8

Wang, T.-C., Chen, Y.-H., 2008. Applying fuzzy linguistic preference relations to the improvement of consistency of fuzzy AHP. Inf. Sci. (Ny). 178, 3755–3765. https://doi.org/10.1016/j.ins.2008.05.028

Wang, Y.-M., Luo, Y., Hua, Z., 2008. On the extent analysis method for fuzzy AHP and its applications. Eur. J. Oper. Res. 186, 735–747. https://doi.org/10.1016/j.ejor.2007.01.050

Warren, S.D., Hohmann, M.G., Auerswald, K., Mitasova, H., 2004. An evaluation of methods to determine slope using digital elevation data. CATENA 58, 215–233. https://doi.org/10.1016/j.catena.2004.05.001

Weiss, A.D., 2001. Topographic Position and Landforms Analysis (Conference Poster), in: ESRI International User Conference. p. 2.

Wilson, J.P., Gallant, J.C., 2000. Digital Terrain Analysis, in: Wilson, J.P., Gallant, J.C. (Eds.), Terrain Analysis: Principles and Applications. John Wiley & Sons, Inc, pp. 1–27.

Wolock, D.M., McCabe, G.J., 1995. Comparison of Single and Multiple Flow Direction Algorithms for Computing Topographic Parameters in TOPMODEL. Water Resour. Res. 31, 1315–1324. https://doi.org/10.1029/95WR00471

WOODCOCK, N.H., 1977. Specification of fabric shapes using an eigenvalue method. Geol. Soc. Am. Bull. 88, 1231. https://doi.org/10.1130/0016-7606(1977)88<1231:SOFSUA>2.0.CO;2

Zhang, H., Yao, Z., Yang, Q., Li, S., Baartman, J.E.M., Gai, L., Yao, M., Yang, X., Ritsema, C.J., Geissen, V., 2017. An integrated algorithm to evaluate flow direction and flow accumulation in flat regions of hydrologically corrected DEMs. CATENA 151, 174–181. https://doi.org/10.1016/j.catena.2016.12.009